Desalination and Water Treatment
www.deswater.com

doi: 10.5004/dwt.2017.0237

60 (2017) 301–309
January

Removal of Pb(II) from water by carbonized walnut shell: characterization of adsorbent, adsorption capacity, kinetic, thermodynamic and isotherm studies

Bircan Köse, Saliha Erentürk*

Department of Chemical Engineering, Faculty of Engineering, University of Ataturk, Erzurum, Turkey, emails: serenturk@yahoo.com (S. Erentürk), bircank28@gmail.com (B. Köse)

Received 29 February 2016; Accepted 14 July 2016

ABSTRACT

The aim of this study is to investigate the efficiency of the carbonized walnut shell (CWS) as adsorbent on the removal of Pb(II) from an aqueous solution. Walnut shell was carbonized in a 500°C heated oven passing N_2 and then characterized by using Brunauer–Emmett–Teller (BET), scanning electron microscopy and Fourier transform infrared spectroscopy (FT-IR). The specific surface area of the sample is 431.99 m^2/g. Adsorption of Pb(II) by various batch experimental conditions such as pH (1.2–6), temperature (26°C, 37°C and 45°C), adsorbent dose (0.4, 0.8, 1 g/L) and metal ion concentrations (50–150 mg/L) was investigated. The maximum adsorption capacity of CWS was obtained as 120.48 mg/g. Three empirical adsorption models (i.e., Langmuir, Freundlich and Temkin) were used for the evaluation of the adsorption equilibrium data. The equilibrium data fitted very well with all of the investigated isotherm models. The adsorption results were also investigated in terms of kinetic and thermodynamic. The kinetic studies showed that the better applicability for the adsorbent was the pseudo-second-order model. The thermodynamic parameters, such as Gibb's free energy change ($\Delta G°$), standard enthalpy change ($\Delta H°$) and standard entropy change ($\Delta S°$), were also evaluated. The results of the thermodynamic parameters ($\Delta G° < 0$, $\Delta S = 40.81$ J/mol/K, $\Delta H° = 9.45$ kJ/mol) showed that the adsorptions were spontaneously endothermic reactions.

Keywords: Pb(II); Adsorption; Kinetic; Isotherm; Thermodynamic

1. Introduction

The rapidly growing industrialization and the production with an increasing consumer demand have led to heavy metal emissions. Heavy metals are generally recognized as a threat toward human health and ecosystems because of their high environmental pollutant and toxic and carcinogenic characteristics [1]. Among all the heavy metals, lead is a carcinogenic and non-biodegradable substance, and it is commonly used in many industrial applications such as textile, petroleum refining, tanneries, storage battery manufacturing, fuels, explosive manufacturing, photographic materials, coating, aeronautical, automobile, mineral processing and steel industries [2]. These industries may lead to contamination of the surface and ground water with Pb(II) ions. The presence of lead, even in low concentrations, in drinking water could lead to accumulations of lead in the body, and this can cause anemia, kidney malfunction, tissue damage of brain and even death [1–6].

The removal of lead from water is an important issue, and there are various methods to solve this problem such as chemical precipitation, ionic exchange, filtration, electrochemical treatment, membrane techniques and recovery by evaporation and adsorption [7–9]. All these methods except adsorption are used only in special cases because they are either economically unfavorable or technically complicated.

The adsorption method allows the evaluation of many waste materials. The adsorbents, which are used in the adsorption, provide low costs, and they are readily available materials,

* Corresponding author.

which are usually produced from the natural materials comprising the carbon structure such as agricultural wastes [10].

Although a number of studies have been conducted on the removal of metal ions from aqueous solutions using various adsorbents such as shells of hazelnut and almond [11]; mistalea (*Viscum album L.*) [12]; walnut, hazelnut, almond, pistachio shell, and apricot stone [10]; *Melocanna baccifera Roxburgh* (bamboo) [13]; bael leaves (*Aegle marmelos*) [4]; hazelnut husks [14]; modifying walnut shell [15]; walnut shells and jujube seeds [16]; citric acid modified pine sawdust [17]; sunflower seed hull [18], palm tree fronds [19]; walnut and poplar woods [20]; and tea waste biomass [21], every special material needs to be given a particular focus for investigation.

The aim of this study is to investigate the removal of Pb(II) ions from aqueous solution by using an adsorbent obtained from walnut shell, which is manufactured relatively easy and low cost. The walnut shell used as an adsorbent in this study is an agricultural waste product particularly in the Anatolian part of Turkey. Although walnut shell is considered as an agricultural waste product generally and is consumed as burn-material in Turkey, from the economical point of view, walnut shell can also be used as an alternative approach to activated carbon for the adsorption process. The main advantage of Pb(II) removal by using walnut shell is that it is in plenty and easy availability. This makes it a strong choice in the investigation of an economic way of Pb(II) removal. Considering previous works, we performed a different experimental approach and method to remove Pb(II) from aqueous solutions without any chemical treatment.

The adsorbent obtained from the walnut shell was characterized by using Fourier transform infrared spectroscopy (FT-IR), scanning electron microscopy (SEM) and Brunauer–Emmett–Teller (BET). Effects of solution pH, adsorbent dose, initial metal concentration and adsorption temperature on Pb(II) ions adsorption were studied in detail. The adsorption equilibrium data were analyzed using Langmuir, Freundlich and Temkin isotherms. Pseudo-first-order and pseudo-second-order models were used for investigation of the adsorption kinetic.

2. Materials and methods

2.1. Preparation of the adsorbent

Walnut shells were used as initial raw materials. These are grown in Tortum, which is a city in Erzurum, Turkey. Firstly, the walnut shells were broken. Secondly, the walnut shells were burned in the furnace at the nitrogen gas flow rate of 58 L/h. They were heated from room temperature to 500°C with the heating rate of 10°C/min. The temperature of 500°C was kept for 90 min. After the end of the carbonization, the nitrogen gas passed continuously until it returns to room temperature. Finally, the samples obtained were milled and sieved to get the carbon particles with the diameter smaller than 0.092–0.063 mm. Carbonized walnut shell (CWS) was characterized by BET, SEM and FT-IR analysis.

2.2. Batch experiments

The stock solution containing 1,000 mg/L of Pb(II) ions was prepared by dissolving an sensitive quantity of $Pb(NO_3)_2$ in distilled water. The test solutions used in the experiments were prepared by diluting from the stock solution. The test chemicals were pure as analytical and supplied by Merck (Germany). The batch adsorption experiments were carried out on a thermostatic incubator shaker with a shaking speed of 200 rpm. All mixtures, after adsorption experiments were filtered through Sartorious Stedim 391 to obtain clear solutions, after the adsorption experiments. The concentration of the residual Pb(II) ions in the solution was measured by atomic absorption spectrophotometer (Shimadzu AA-670, USA) at 283.3 nm.

The following equation had been utilized to find the removal efficiency of Pb(II) ion:

$$\%\ \text{Removal efficiency} = \frac{C_0 - C_e}{C_0} \times 100 \tag{1}$$

The following equation was used to find the equilibrium amount of lead adsorbed:

$$q_e = \frac{(C_0 - C_e)V}{m} \tag{2}$$

where q_e is the amount of ions adsorbed per mass unit of adsorbent (mg/g); C_0 is the initial concentrations (mg/L); C_e is the final concentrations (mg/L); V is the volume of the solution (L) and m is the mass of adsorbents (g).

2.3. Adsorption thermodynamic

Thermodynamic parameters are useful in defining whether the adsorption is endothermic or exothermic, and in determining the spontaneity of the adsorption process.

The values of the enthalpy, $\Delta H°$; the entropy, $\Delta S°$ and the Gibbs free energy, $\Delta G°$ for Pb(II) ions adsorption onto CWS were obtained in this study. The amounts of $\Delta H°$ and $\Delta S°$ can be calculated from the slopes and intercepts of the straight line obtained from the plot of $\ln K_d$ vs. $1/T$ by using Eq. (3) [22]:

$$\ln K_d = \frac{\Delta S°}{R} - \frac{\Delta H°}{RT} \tag{3}$$

$$K_d = \frac{q_e}{C_e} \tag{4}$$

where K_d (l/g) is the distribution coefficient; R (8.314 J/mol/K) is the gas constant and T (K) is the absolute temperature of the aqueous solution [22]. The value of K_d was calculated at different temperature and at equilibrium time using Eqs. (2) and (4).

After obtaining $\Delta H°$ and $\Delta S°$ values of the adsorption, $\Delta G°$ of each temperature was calculated with the following equation:

$$\Delta G° = \Delta H° - T\Delta S° \tag{5}$$

2.4. Adsorption isotherm models

The adsorption equilibrium data of Pb(II) ions onto the CWS were analyzed in terms of Langmuir, Freundlich and Temkin isotherm models. The optimal isotherm data were

obtained by plotting the amount of Pb(II) ions adsorbed per mass unit of the adsorbent (mg/g) against the concentration of Pb(II) ions remaining in the solution (mg/L), which was shown in Fig. 8.

The Langmuir adsorption isotherm [23] presumes that adsorption occurs at specific homogenous sites within the adsorbent and makes the prediction of adsorption capacities under various conditions. The linear form of the Langmuir isotherm can be described as follows:

$$\frac{C_e}{q_e} = \frac{1}{Q_m b} + \frac{C_e}{Q_m} \tag{6}$$

where q_e is the adsorption capacity at equilibrium (mg/g); Q_m is the maximum monolayer adsorption capacity (mg/g); b is the Langmuir constant related to the affinity of Pb(II) ions to the CWS (l/mg) and C_e is the concentration of the Pb(II) ions in the solution at equilibrium (mg/L) [24].

The Freundlich adsorption isotherm [23] can be applied to non-ideal sorption on heterogeneous surfaces as well as multi-layer sorption and is expressed by the following equation:

$$q_e = K_f C_e^{1/n} \tag{7}$$

The linear form of Freundlich isotherm is as follows:

$$\ln q_e = \ln K_f + \frac{1}{n}\ln C_e \tag{8}$$

where K_f is the Freundlich constant ((mg/g) (L/mg)$^{(1/n)}$) related to the bonding energy, and n is a measure of the deviation from the linearity of the adsorption (g/L) [24].

The Temkin adsorption isotherm contains a factor that explicitly taking into the account of adsorbent–adsorbate interactions. By ignoring the extremely low and large value of concentrations, the model assumes that heat of adsorption (function of temperature) of all molecules in the layer would decrease linearly rather than logarithmic with coverage [23]. The model is given by the following equation:

$$q_e = \frac{RT}{b}\ln(K_T C_e) = B\ln(K_T C_e) \tag{9}$$

where R is the gas constant (8.314 J/mol/K); T is the temperature (K); K_T is the equilibrium binding constant (L/mg) corresponding to the maximum binding energy; $B = RT/b$ is the constant related to the heat of adsorption and b is the heat of the adsorption (J/mol) [24].

The dimensionless parameter (R_L) value, which is defined in Eq. (10) is used to determine the above-mentioned values b and C_0 [1,23,25].

$$R_L = \frac{1}{1 + bC_o} \tag{10}$$

According to dimensionless R_L values, adsorption types are shown in Table 1 [26].

Table 1
According to dimensionless R_L values, given are adsorption types

R_L values	Adsorption type
$R_L > 1$	Unfavorable
$R_L = 1$	Linear
$0 < R_L < 1$	Favorable
$R_L = 0$	Irreversible

2.5. Adsorption kinetics models analysis

Kinetic models were used to determine the control step of the adsorption process. For this purpose, the data obtained from the experiments were analyzed in the pseudo-first-order and pseudo-second-order sorption equations [23,27].

The pseudo-first-order rate expression of Lagergren is given as follows:

$$\log(q_e - q_t) = \log(q_e) - \frac{k_1}{2.303}t \tag{11}$$

where q_t (mg/g) is the amount of the adsorbed Pb(II) ions on the CWS at time t (min), and k_1 (1/min) is the rate constant of the pseudo-first-order adsorption. A straight line is obtained by plotting $\log(q_e - q_t)$ vs. t, and in this way, the adsorption rate constants k_1 and q_e were calculated from the slope and intercept of the line, respectively.

The pseudo-second-order is given as follows [28]:

$$\frac{t}{q_t} = \frac{t}{q_e} + \frac{1}{k_2 q_e^2} \tag{12}$$

where k_2 (g/mg/min) is the rate constant of the pseudo-second-order adsorption. k_2 and q_e were obtained from the intercept and the slope of the plotting t/q_t vs. t. q_e, k_1 and k_2 are demonstrated in Table 6.

3. Results and discussion

3.1. TGA analyzing

The thermal decomposition is offered with the thermogravimetric analysis or thermal gravimetric analysis (TGA) and differential thermal gravimetry (DTG) curves, and these curves are called the experimental and differential thermograms, respectively [22,29]. The thermal decomposition occurs in the structure of walnut shells during carbonization. The TGA and DTG curves were investigated in a nitrogen atmosphere, and they are illustrated at Fig. 1. It was observed a peak caused by moisture at 118°C, and the moisture loss was measured as 2.58% in this area. The removing of volatile has been observed in the area between 270°C and 370°C. The degradation of hemicellulose and cellulose structure were also realized in this area. The total weight reduction in this section was measured as 56.45%. Firstly, hemicellulose components decompose. When it is completed, the degradation of cellulose begins. After 370°C, the weight reduction has slowed and started the degradation of lignin. It was seen from the DTG and TGA curves that the rate of the weight change was constant at temperatures above 500°C.

3.2. Adsorbent characterization

3.2.1. SEM analysis

The SEM micrographs of CWS are shown in Fig. 2. These micrographs revealed that the surface of CWS was highly porous, and the size of the holes was heterogeneous as expected. The surface area of the adsorbent has increased by the porous structure, so that the metal adsorption capacity of the adsorbent was increased [13].

3.2.2. FT-IR spectra

The chemical nature of the adsorbent surface can be defined by FT-IR spectra. The FT-IR spectrum of CWS is shown in Fig. 3. The absorption peaks are indicating the presence of the various functional groups, which can be seen in the spectrum. These peaks can be explained as following. The shoulders observed at 2.850–2.950 cm^{-1} due to aliphatic (C–H) groups and appeared for carbon samples. The bands near 1.600 cm^{-1} are due to C=C stretching vibration in aromatic. The absorption within the range of 1.170–1.070 cm^{-1} can be ascribed to C-C-C bonds [20,23,25].

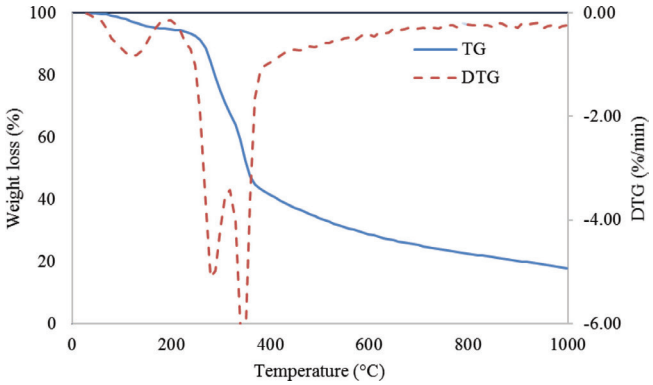

Fig. 1. The thermal decomposition (TG and DTG curves of walnut shells).

3.2.3. Surface area and pore structure

The surface area and the pore structure of CWS were characterized by using the BET. The values of S_{BET}, V_{micro} and V_{meso}, which are obtained from the isotherms of the CWS in a nitrogen atmosphere, are listed in Table 2. The specific surface area of the sample was determined as 431.99 m^2/g. According to the International Union of Pure and Applied Chemistry, the pore structures of carbons are classified into three groups as: micropore (≤2 nm), mesopore (2–50 nm) and macropore (≥50 nm) [30,31]. The micropore volume of CWS is equal to 0.17 cm^3/g, and this quantity corresponds to 82.90% on the whole surface. In addition, the mesopore volume is 0.06 cm^3/g, which corresponds to 25.62%.

3.3. Effect of solution pH

The pH is a very important parameter in an adsorption process. If the pH increases or decreases, the activity of the functional groups of the adsorbent varies. This is responsible for metal adsorption. The pH affects also the competition between H^+ and the metallic ions, which are trying to reach to the active sites of the adsorbent. [32]. In the pH studies, the initial lead concentration was kept constant at 50 mg/L. The test solutions were adjusted to the desired pH (1.2, 3.0, 4.0, 5.0, 6.0). In this test, the adsorbent dose and temperature were constant and selected as 0.4 g/L and 37°C, respectively. The effect of the pH on the removal of Pb(II) ion was illustrated in Fig. 4. In Fig. 4, it can be seen that the amount of lead adsorbed by the CWS increased from 3.5 to 57.2 mg/g with the increasing of the pH value from 1.2 to 5, respectively. The adsorption capacity of CWS reached the maximum value at pH 5.0. Reducing the pH of the solution will result in increasing the number of hydronium ions in the solution. Thus, hydronium ions will surround the surface of the adsorbent and will prevent binding of the metal ions onto the active sites. When the pH increases, the hydronium ions bonded to the active sites will release the surface; thus, metal ions can find the possibilities to binding onto the emptied surface [33].

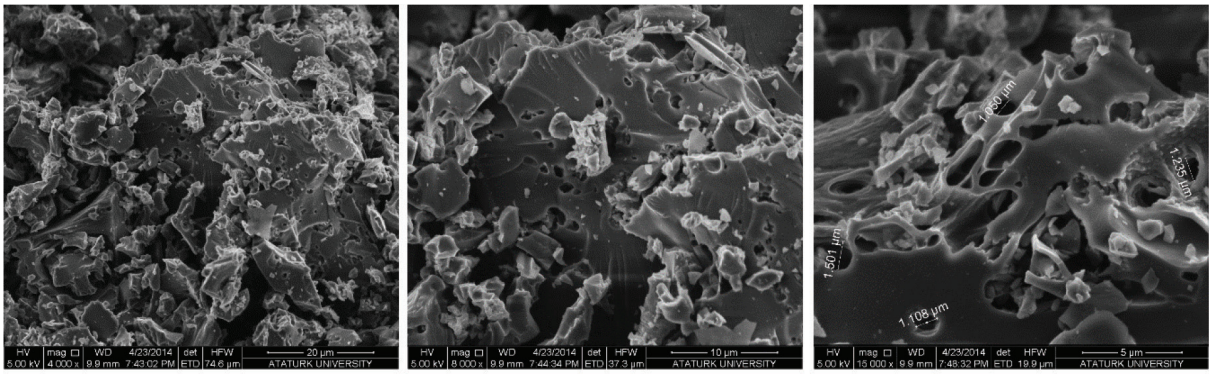

a) HV 5.00kV
mag 4000x
WD 9.9 mm
HFW 74.6 µm
20 µm

b) HV 5.00kV
mag 8000x
WD 9.9 mm
HFW 37.3 µm
10 µm

c) HV 5.00kV
mag 15000x
WD 9.9 mm
HFW 19.9 µm
5 µm

Fig. 2. SEM micrographs of carbonized walnut shell (CWS) (this images were enlarged to: (a) 4000, (b) 8000 and (c) 15000 times).

In addition, the number of H^+ ions competing with the metal ions for binding active sites will decrease within the solution; eventually adsorption of Pb(II) onto adsorbent will increase [1,4]. When the pH value increases above 6.0, the Pb(II) ions will precipitate as hydroxyl forms such as $(Pb(OH))^+$, $(Pb_3(OH)_4)^+$ and $(Pb(OH)_2)$ [12,33,34]. In order to prevent precipitation of Pb(II) ions, all the following experiments were conducted at pH 5.0.

3.4. Effect of adsorbent dose on Pb(II) adsorption

In adsorbent dose studies, the solution of the pH and initial concentration was kept constant at 5 and 50 mg/L, respectively. In order to investigate the effect of the adsorbent dose on Pb(II) adsorption, the amounts of CWS were selected as 0.4, 0.8 and 1 g/L, and the temperature was kept constant at 37°C during the experiments. The results were illustrated in Fig. 5.

It can be seen from Fig. 5 that there is an increase in the percentage removal of Pb(II) when the adsorbent dose were increased. After the adsorbent dose was varied from 0.4 to 1 g/L, the adsorption percentage increased from 57.19% to 89.81%. The adsorbent dose were found to be significant in the adsorption of Pb(II).

When the adsorbent dose increases, the number of the active sites in the solution will increase. This resulted in decreasing the competition between the molecules for binding sites [34]. Although the percentage removal of Pb(II) increased with the increasing in the adsorbent dose, the adsorption capacity (q_e) is reduced. Similar results about the adsorbent dose in the adsorption of Pb(II) have been reported by various investigators in the literatures [1,34,35]. Besides that, if a higher dose of the adsorbent is used, the adsorbents can be agglomerated. This situation can be lead to decline on the total surface area and subsequent to a reduction of adsorption [1].

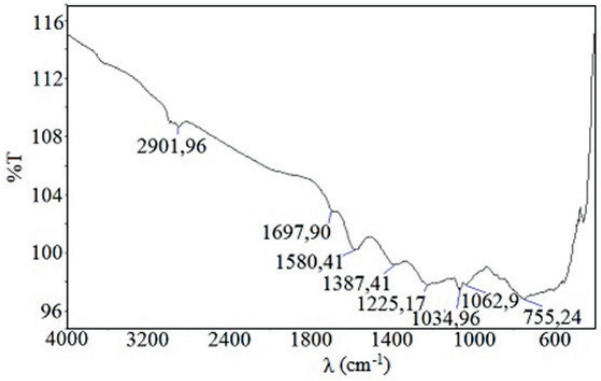

Fig. 3. FT-IR spectrum of CWS.

3.5. Effect of initial Pb(II) concentration on adsorption

The effect of the initial Pb(II) ion concentration varied from 50 to 150 mg/L on the adsorption of Pb(II) onto the CWS was investigated at the temperature of 37°C, the pH of 5.0 and the adsorbent dose of 0.4 g/L. The results were illustrated in Fig. 6. While the initial Pb(II) concentration were increased from 50 to 150 mg/L, the percentage removal of Pb(II) were decreased from 57.19% to 29.71%. However, the adsorption capacity were increased from 63.61 to 102.27 mg/g. The decreasing of the percentage removal of Pb(II) was due to the presence of the excess amount of Pb(II) in the solution.

Increasing the adsorption capacity can be attributed to the utilization of all existing active sites for adsorption at higher Pb(II) concentration [14,24,36].

The initial solution concentration provides the required driving force to overcome the resistance of the mass transfer

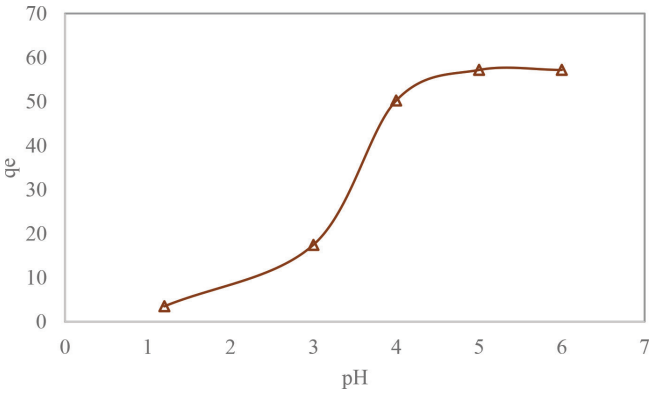

Fig. 4. The effect of pH on the removal of lead with CWS (initial concentration = 50 mg/L; contact time = 90 min, T = 37°C).

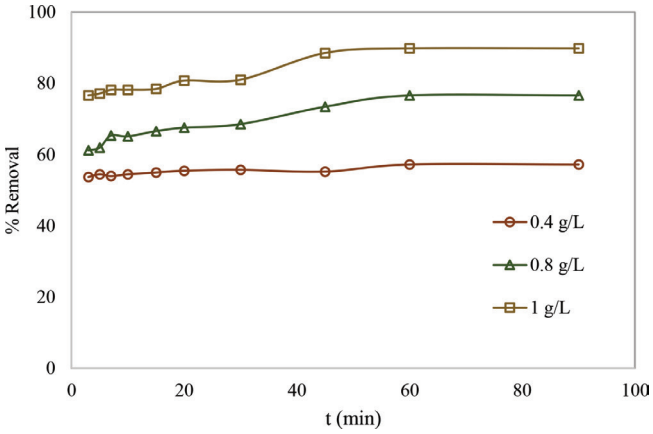

Fig. 5. The effect of the adsorbent dosage on Pb(II) adsorption (pH = 5.0, initial concentration = 50 mg/L, T = 37°C).

Table 2
Brunauer–Emmett–Teller (BET) surface area and pore size distributions of the adsorbent derived from walnut shell

S_{BET}	S_{micro}		S_{meso}		V_{Total}	V_{micro}		V_{meso}	
(m^2/g)	(m^2/g)	(%)	(m^2/g)	(%)	(cm^3/g)	(cm^3/g)	(%)	(cm^3/g)	(%)
431.99	358.13	82.90	73.86	17.10	0.22	0.17	74.38	0.06	25.62

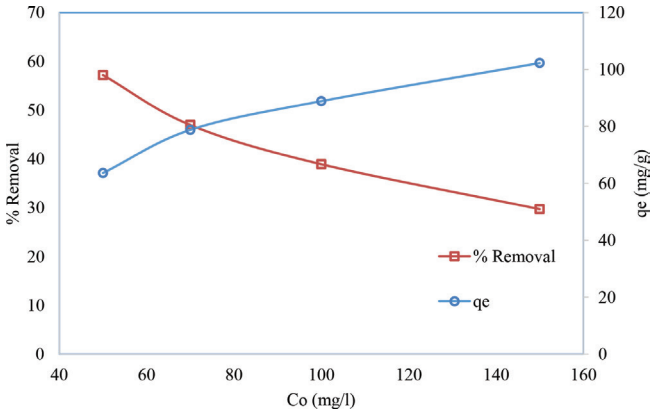

Fig. 6. The effect of the initial concentration on Pb(II) adsorption (pH = 5.0, adsorbent dosage = 0.4 g/L, T = 37°C).

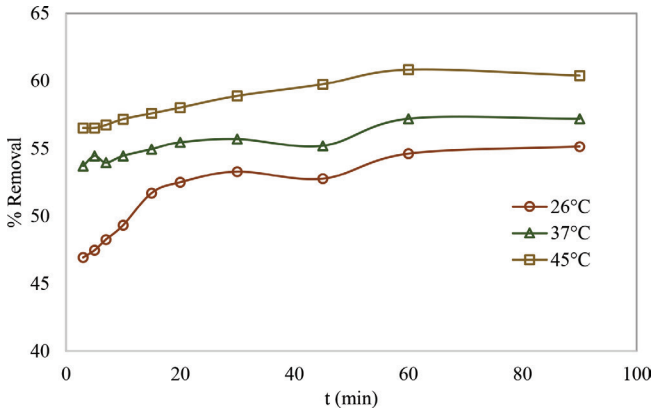

Fig. 7. The effect of temperature on Pb(II) adsorption (pH = 5.0, adsorbent dosage = 0.4 g/L, initial concentration = 50 mg/L).

from the aqueous phase to the surface of the adsorbent, which contains the active binding site. In order to occur the adsorption process, adsorbate molecules must move from the bulk solution to the exterior surface of the adsorbent and then from the exterior surface to the pores of the adsorbent. Therefore, the increase in the initial solution concentration can improve the interaction between Pb(II) and the CWS, which results in the increase of adsorption capacity of Pb(II) [14,24,36].

3.6. Effect of the temperature

In order to investigate the effect of the temperature, three different temperatures were selected as parameters such as 26°C, 37°C and 45°C. During the experiments, the other parameters were kept constant like the adsorbent dose 0.4 g/L, pH 5.0, the initial Pb(II) ion concentration 50 mg/L. The effect of the temperature was illustrated in Fig. 7. It was seen from Fig. 7 that the percentage removal of Pb(II) increased from 54.6 to 60.8 when the temperatures were raised from 26°C to 45°C, respectively. It was also seen from Fig. 7 that the adsorption was endothermic. When the temperature increases, the molecular mobility will also increase. As a result of the increasing molecular mobility, the diffusion of the adsorbate having the drag force of the metal ions throughout the pores within the adsorbent will increase too. When the temperature increases, some internal bonds near the active surface sites of the adsorbent are broken, and new active sites are formed. Hereby, the adsorption of metal ions increases with the increase in temperature. The increase in adsorption with temperature may also be attributed to the decrease in the boundary layer thickness surrounding the sorbent with increasing temperature, as a result the mass transfer resistance of adsorbate in the boundary layer decreases [9,37,38].

3.7. Thermodynamic study

The thermodynamic parameters, such as the Gibb's free energy change ($\Delta G°$), the standard enthalpy change ($\Delta H°$) and the standard entropy change ($\Delta S°$) were evaluated in this section. All the thermodynamic parameters were listed in Table 3. The values of ($\Delta H°$) and ($\Delta S°$) were obtained from Van 't Hoff equation (Eq. (3)). As the $\Delta G°$ values were

Table 3
Thermodynamic parameters for the adsorption of Pb(II)

T, °C	K_d	$\Delta G°$, kJ/mol	$\Delta S°$, J/mol.K	$\Delta H°$ kJ/mol
26	3.07	–2.75		
37	3.34	–3.20	40.81	9.45
45	3.88	–3.53		

negative, it can be said that the adsorption process of Pb(II) was spontaneous under the studied conditions. The values of $\Delta G°$ decreased from –2.75 to –3.53 kJ/mol in the temperature range of 26°C–45°C, indicating that the spontaneity of the adsorption reaction was enhanced with the rising temperature. The value of enthalpy change $\Delta H°$ was positive for Pb(II) adsorption, suggesting the endothermic nature of the reaction. While an exothermic adsorption process indicates either physical or chemical sorption, the endothermic process can be attributed to the chemisorption. Therefore, the positive enthalpy value obtained from this study confirms that the adsorption of Pb(II) onto the CWS is controlled by chemical adsorption rather than physical adsorption. The positive entropy change $\Delta S°$ suggested that the degree of disorder increased with the increase of species number at the solid/liquid interface. When the Pb(II) ions were adsorbed by the adsorbent, the number of Pb(II) ions in the solutions will decrease. As a result of this, the randomness that causes an increase in the entropy of the solution will increase [39].

3.8. Adsorption isotherms

The equilibrium behaviors of the adsorbate uptake was described by adsorption isotherms. For isotherms experiments, solutions containing 50, 70, 100 and 150 mg/L Pb(II) initial concentrations were prepared. Before the experiments, the pH of the solutions were adjusted to 5, and then 0.4 g/L of adsorbent was added into each solution and was stirred at 200 rpm for 90 min at 37°C temperature. The amounts of Pb(II) extracted at equilibrium, q_e (mg/g), were calculated according to Eq. (2) [40]. The Langmuir, Freundlich and Temkin models were applied to experimental data. The isotherm data were obtained by plotting amount of lead adsorbed on the solid (mg/g) against the remaining concentration of lead in the solution (mg/L).

The equilibrium adsorption isotherms are shown in Fig. 8, and regression coefficients are given in Table 4. It can be seen from Table 4 that the correlation coefficients were above 0.99 for all of the isotherm models. It can be said that the equilibrium data were suitable for all of the isotherm models when the correlation coefficients between the experimental results and the model data were considered. A close look at the obtained regression values obtained indicates that Langmuir, Freundlich and Temkin models investigated in this study are almost equally applicable [40,41,25]. In this study, The R_L value was obtained in the range of 0–1, which is favorable for the adsorption of Pb(II) at studied conditions (Table 1).

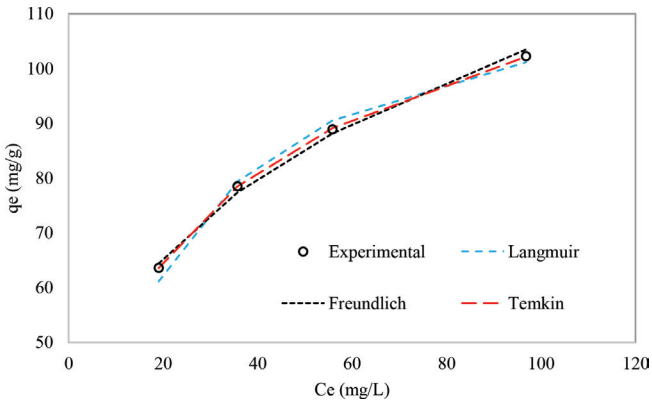

Fig. 8. The comparative results of the adsorption isotherm models in the adsorption of Pb(II) onto CWS (adsorbent dose = 0.4 g/L, pH = 5; T = 37°C).

The results of the maximum monolayer adsorption capacity (Q_m) for Pb(II) ions onto the CWS with other adsorbents are shown in Table 5. When the testing conditions are the exactly same with others testing conditions, the maximum adsorption capacities of this study can be compared by other studies. Otherwise, it does not reflect the realities to make comparisons. Because, the adsorption capacities vary depending on the test conditions. Therefore, studies, which made with similar conditions, have been selected for comparison. These studies are given in Table 5.

3.9. Adsorption kinetics

The prediction of the order of the adsorption rate kinetics and the adsorption rate constants is an important step for the design of an adsorption system and to evaluate the basic qualities of the good adsorbent. The data obtained from the effect of the contact time on the adsorption process can be used to find which of the kinetics models can define better the adsorption of Pb(II) ions onto the CWS. For this purpose, the kinetic model studies were carried out for the adsorption of Pb(II) onto the CWS with for pseudo-second-order expression and pseudo-first-order expression. The experimental data were obtained at 1, 3, 5, 7, 10, 15, 20, 30, 45, 60 and 90 min for using in the kinetic studies. The linearized form of the pseudo-first-order model and the pseudo-second-order model for the adsorption of Pb(II) ions onto CWS is given in Figs. 9 and 10, respectively.

The obtained kinetic model parameters by linear regressions were given in Table 6. From Table 6, it was observed that the better R^2 values were observed for the pseudo-second-order kinetic model than the pseudo-first-order kinetic model, which indicates that the pseudo-second-order

Table 4
The isotherms model constants for Pb(II) ions adsorption onto carbonized walnut shell (CWS)

Langmuir constants			Freundlich constants			Temkin constants		
Q_m (mg/g)	b (L/mg)	R^2	K_f ((mg/g) (L/mg)$^{(1/n)}$)	n	R^2	B	K_T (L/mg)	R^2
120.482	0.0541	0.998	27.2649	3.428	0.995	23.732	0.765	0.999

Table 5
Comparison of the Langmuir adsorption capacities (Q_m) of various adsorbents used for the adsorption of Pb(II) ions

Adsorbent	T (°C)	m (g/L)	C_0 (mg/L)	Q_m (mg/g)	References
CWS	37	0.4	50–150	120.48	This study
DAT and DAT-HDTMABr (surfactant-modified diatomaceous earth)	35	4	10–200	11.962 and 16.578	[42]
Activated carbon developed from water hyacinth (chemical activation with H_3PO_4)	25	1	1–200	118.8	[1]
Coal olive stone activated carbon (COSAC) (activated carbon derived from olive stones)	30	1.2	104–1040	148.77	[43]
Activated carbon developed from Apricot stone (chemical activation with sulphuric acid)	20	1	10–100	21.38	[44]
Melocanna baccifera raw charcoal (MBRC) and *Melocanna baccifera* activated charcoal (MBAC)	29	1	50–90	10.66 and 53.76	[13]
Bael leaves (*Aegle marmelos*)	25	0.1	8.7–180.2	125	[4]
Activated carbon prepared from *Phaseolus aureus* hulls	30	0.5	20–250	21.8	[23]

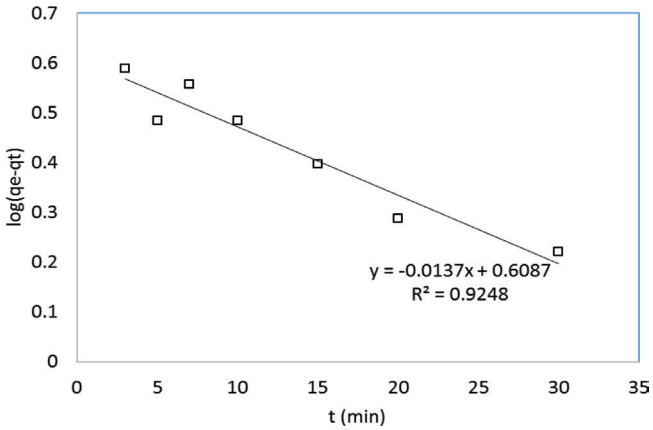

Fig. 9. Plot of the pseudo-first-order kinetics model of Pb(II) removal by CWS (adsorbent dosage = 0.4 g/L, pH = 5; T = 37°C, initial concentration = 50 mg/L).

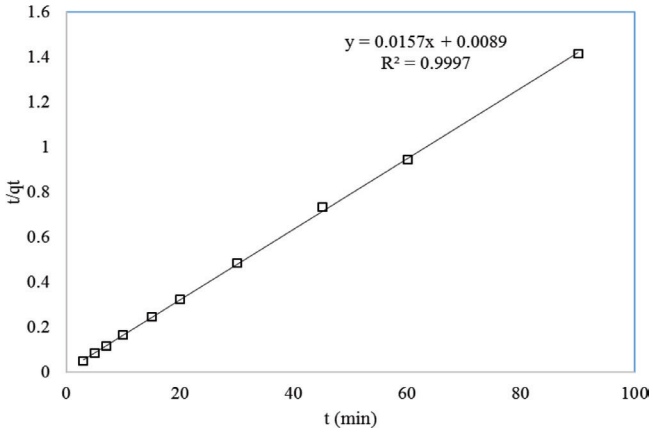

Fig. 10. Plot of the pseudo-second-order kinetics model of Pb(II) removal by CWS (adsorbent dosage = 0.4 g/L, pH = 5; T = 37°C, initial concentration = 50 mg/L).

Table 6
Adsorption rate constants associated with the pseudo-first- and the pseudo-second-order kinetic models

	$q_{e,experimental}$ (mg/g)	R^2	$q_{e,calculated}$ (mg/g)	k_1 1/min	k_2 g/mg/min
Pseudo-first–order kinetic model	63.61	0.9248	4.062	0.0316	–
Pseudo-second-order kinetic model	63.61	0.9997	63.694	–	0.0277

kinetic model fits the adsorption kinetic data better than the pseudo-first-order kinetic model. The values of R^2 were found to pseudo-second-order and pseudo-first-order expression as 0.9997 and 0.9248, respectively. Thus, the adsorption of Pb(II) ions onto the CWS was represented by the pseudo-second-order kinetic model. This result indicates that the adsorption rate may be controlled by chemical adsorption, which provides the best correlation of the experimental data. In the chemical adsorption, the valency forces involve through sharing or exchange of electrons between the adsorbent and adsorbate. This means that the adsorption process between adsorbent active sites and Pb(II) can be achieved by chemical interaction including ionic or covalent bonds [18,24].

4. Conclusion

In this study, walnut shell was prepared by the carbonization and then used for the Pb(II) ions adsorption as an adsorbent. The adsorbent had highly heterogeneous porous sizes, and its specific surface area was obtained as 431.99 m^2/g. The CWS exhibited a high adsorption capacity for Pb(II). It is said from the results of this study that Pb(II) adsorption on the CWS was strongly influenced by adsorbent dose, initial metal concentration, pH and temperature.

The results show that increasing the initial pH, the adsorption capacity passes through an extremum at alkaline pH for the alkaline activated carbon. Increasing the initial lead concentration decreases the percentage removal but it increases the sorption capacity for the CWS. Three empirical adsorption isotherm models (Langmuir, Freundlich and Temkin) were used for the evaluation of the adsorption equilibrium data. When the correlation coefficients between the experimental results and model data were considered, it can be said that the equilibrium data fitted very well with the correlation coefficients of above 0.99 for all of the isotherm models investigated. The kinetic studies showed that the adsorption of Pb(II) onto the CWS followed a pseudo-second-order kinetics. The adsorption thermodynamic showed that the adsorption process was endothermic and spontaneous in nature.

Acknowledgment

This work was supported by the Atatürk University Research Foundation (BAP, 2013/108).

References

[1] Y. Huang, S.X. Li, J.H. Chen, X.L. Zhang, Y.P. Chen, Adsorption of Pb(II) on mesoporous activated carbons fabricated from water hyacinth using H_3PO_4 activation: adsorption capacity, kinetic and isotherm studies, Appl. Surf. Sci., 293 (2014) 160–168.
[2] M. Naushad, Z.A. ALOthman, M.R. Awual, M.M. Alam, G.E. Eldesoky, Adsorption kinetics, isotherms, and thermodynamic studies for the adsorption of Pb^{2+} and Hg^{2+} metal ions from aqueous medium using Ti(IV) iodovanadate cation exchanger, Ionics, 21 (2015) 2237–2245.
[3] M. Machida, B. Fotoohi, Y. Amamo, L. Mercier, Cadmium(II) and lead(II) adsorption onto hetero-atom functional mesoporous silica and activated carbon, Appl. Surf. Sci., 258 (2012) 7389–7394.
[4] S. Chakravarty, A. Mohanty, T.N. Sudha, A.K. Upadhyay, J. Konar, J.K. Sircar, A. Madhukar, K.K. Gupta, Removal of Pb(II) ions from aqueous solution by adsorption using bael leaves (*Aegle marmelos*), J. Hazard. Mater., 173 (2010) 502–509.
[5] P. Tan, J. Sun, Y. Hu, Z. Fang, Q. Bi, Y. Chen, J. Cheng, Adsorption of Cu^{2+}, Cd^{2+} and Ni^{2+} from aqueous single metal solutions on graphene oxide membranes, J. Hazard. Mater., 297 (2015) 251–260.
[6] M. Naushad, Z.A. ALOthman, Inamuddin, H. Javadian, Removal of Pb(II) from aqueous solution using ethylene

diamine tetra acetic acid-Zr(IV) iodate composite cation exchanger: kinetics, isotherms and thermodynamic studies, J. Ind. Eng. Chem., 25 (2015) 35–41.
[7] M. Naushad, Z.A. ALOthman, G. Sharma, Inamuddin, Kinetics, isotherm and thermodynamic investigations for the adsorption of Co(II) ion onto crystal violet modified amberlite IR-120 resin, Ionics, 21 (2015) 1453–1459.
[8] Z.E. Kul, Y. Nuhoğlu, S. Kul, Ç. Nuhoğlu, F.E. Torun, Mechanism of heavy metal uptake by electron paramagnetic resonance and FTIR: enhanced manganese(II) removal onto waste acorn of *Quercus ithaburensis*, Sep. Sci. Technol., 51 (2016) 115–125.
[9] V.K. Gupta, A. Rastogi, Biosorption of hexavalent chromium by raw and acid-treated green alga *Oedogonium hatei* from aqueous solutions, J. Hazard. Mater., 163 (2009) 396–402.
[10] M. Kazemipour, M. Ansari, S. Tajrobehkar, M. Majdzadeh, H.R. Kermani, Removal of lead, cadmium, zinc, and copper from industrial wastewater by carbon developed from walnut, hazelnut, almond, pistachio shell, and apricot stone, J. Hazard. Mater., 150 (2008) 322–327.
[11] Y. Bulut, Z. Tez, Adsorption studies on ground shells of hazelnut and almond, J. Hazard. Mater., 149 (2007) 35–41.
[12] S. Erenturk, E. Malkoc, Removal of lead(II) by adsorption onto *Viscum album L.*: effect of temperature and equilibrium isotherm analyses, Appl. Surf. Sci., 253 (2007) 4727–4733.
[13] H. Lalhruaitluanga, K. Jayaram, M.N. Prasad, K.K. Kumar, Lead(II) adsorption from aqueous solutions by raw and activated charcoals of *Melocanna baccifera Roxburgh* (bamboo) – a comparative study, J. Hazard. Mater., 175 (2010) 311–318.
[14] M. Imamoglu, A. Vural, H. Altundag, Evaluation of adsorptive performance of dehydrated hazelnut husks carbon for Pb(II) and Mn(II) ions, Desal. Wat. Treat., 52 (2013) 7241–7247.
[15] J.S. Cao, J.X. Lin, F. Fang, M.T. Zhang, Z.R. Hu, A new absorbent by modifying walnut shell for the removal of anionic dye: kinetic and thermodynamic studies, Bioresour. Technol., 163 (2014) 199–205.
[16] W. Bae, J. Kim, J. Chung, Production of granular activated carbon from food-processing wastes (walnut shells and jujube seeds) and its adsorptive properties, J. Air Waste Manage. Assoc., 64 (2014) 879–886.
[17] Y. Zhou, R. Zhang, X. Gu, J. Lu, Adsorption of divalent heavy metal ions from aqueous solution by citric acid modified pine sawdust, Sep. Sci. Technol., 50 (2015) 245–252.
[18] Z. Zou, Y. Tang, C. Jiang, J. Zhang, Efficient adsorption of Cr(VI) on sunflower seed hull derived porous carbon, J. Environ. Chem. Eng., 3 (2015) 898–905.
[19] M. Shoaib, H.M. Al-Swaidan, Optimization and characterization of sliced activated carbon prepared from date palm tree fronds by physical activation, Biomass Bioenergy, 73 (2015) 124–134.
[20] B. Heibati, S. Rodriguez-Couto, M.A. Al-Ghouti, M. Asif, I. Tyagi, S. Agarwal, V.K. Gupta, Kinetics and thermodynamics of enhanced adsorption of the dye AR 18 using activated carbons prepared from walnut and poplar woods, J. Mol. Liq., 208 (2015) 99–105.
[21] A. Gupta, C. Balomajumder, Simultaneous adsorption of Cr(VI) and phenol onto tea waste biomass from binary mixture: multicomponent adsorption, thermodynamic and kinetic study, J. Environ. Chem. Eng., 3 (2015) 785–796.
[22] D. Ding, Y. Zhao, S. Yang, W. Shi, Z. Zhang, Z. Lei, Y. Yang, Adsorption of cesium from aqueous solution using agricultural residue – walnut shell: equilibrium, kinetic and thermodynamic modeling studies, Water Res., 47 (2013) 2563–2571.
[23] M.M. Rao, D.K. Ramana, K. Seshaiah, M.C. Wang, S.W. Chien, Removal of some metal ions by activated carbon prepared from *Phaseolus aureus* hulls, J. Hazard. Mater., 166 (2009) 1006–1013.
[24] U. Pearlin Kiruba, P. Senthil Kumar, K. Sangita Gayatri, S. Shahul Hameed, M. Sindhuja, C. Prabhakaran, Study of adsorption kinetic, mechanism, isotherm, thermodynamic, and design models for Cu(II) ions on sulfuric acid-modified Eucalyptus seeds: temperature effect, Desal. Wat. Treat., 56 (2014) 2948–2965.
[25] N. Esfandiar, B. Nasernejad, T. Ebadi, Removal of Mn(II) from groundwater by sugarcane bagasse and activated carbon (a comparative study): application of response surface methodology (RSM), J. Ind. Eng. Chem., 20 (2014) 3726–3736.
[26] T.H. Ibrahim, Z.B. Babar, M.I. Khamis, Removal of lead (II) ions from aqueous solution using eggplant peels activated charcoal, Sep. Sci. Technol., 50 (2014) 91–98.
[27] V.K. Gupta, A. Rastogi, Equilibrium and kinetic modelling of cadmium(II) biosorption by nonliving algal biomass *Oedogonium sp.* from aqueous phase, J. Hazard. Mater., 153 (2008) 759–766.
[28] X. Ma, X. Liu, D.P. Anderson, P.R. Chang, Modification of porous starch for the adsorption of heavy metal ions from aqueous solution, Food Chem., 181 (2015) 133–139.
[29] T.S. Anirudhan, S.S. Sreekumari, Adsorptive removal of heavy metal ions from industrial effluents using activated carbon derived from waste coconut buttons, J. Environ. Sci., 23 (2011) 1989–1998.
[30] Z.A. ALOthman, M. Naushad, R. Ali, Kinetic, equilibrium isotherm and thermodynamic studies of Cr(VI) adsorption onto low-cost adsorbent developed from peanut shell activated with phosphoric acid, Environ. Sci. Pollut. Res., 20 (2013) 3351–3365.
[31] Z.A. Othman, R. Ali, M. Naushad, Hexavalent chromium removal from aqueous medium by activated carbon prepared from peanut shell: adsorption kinetics, equilibrium and thermodynamic studies, Chem. Eng. J., 184 (2012) 238–247.
[32] M. Sekar, V. Sakthi, S. Rengaraj, Kinetics and equilibrium adsorption study of lead(II) onto activated carbon prepared from coconut shell, J. Colloid Interface Sci., 279 (2004) 307–313.
[33] A.M. Youssef, A.I. Ahmed, M.I. Amin, U.A. El-Banna, Adsorption of lead by activated carbon developed from rice husk, Desal. Wat. Treat., 54 (2014) 1694–1707.
[34] A. Bhat, G.B. Megeri, C. Thomas, H. Bhargava, C. Jeevitha, S. Chandrashekar, G.M. Madhu, Adsorption and optimization studies of lead from aqueous solution using *γ-Alumina*, J. Environ. Chem. Eng., 3 (2015) 30–39.
[35] S. Saadat, A. Karimi-Jashni, M.M. Doroodmand, Synthesis and characterization of novel single-walled carbon nanotubes- doped walnut shell composite and its adsorption performance for lead in aqueous solutions, J. Environ. Chem. Eng., 2 (2014) 2059–2067.
[36] P.S. Kumar, S. Ramalingam, S.D. Kirupha, A. Murugesan, T. Vidhyadevi, S. Sivanesan, Adsorption behavior of nickel(II) onto cashew nut shell: equilibrium, thermodynamics, kinetics, mechanism and process design, Chem. Eng. J., 167 (2011) 122–131.
[37] K.K. Singh, S.H. Hasan, M. Talat, V.K. Singh, S.K. Gangwar, Removal of Cr (VI) from aqueous solutions using wheat bran, Chem. Eng. J., 151 (2009) 113–121.
[38] J. Acharya, J.N. Sahu, B.K. Sahoo, C.R. Mohanty, B.C. Meikap, Removal of chromium(VI) from wastewater by activated carbon developed from Tamarind wood activated with zinc chloride, Chem. Eng. J., 150 (2009) 25–39.
[39] J. Shu, Z. Wang, Y. Huang, N. Huang, C. Ren, W. Zhang, Adsorption removal of Congo red from aqueous solution by polyhedral Cu_2O nanoparticles: kinetics, isotherms, thermodynamics and mechanism analysis, J. Alloys Compd., 633 (2015) 338–346.
[40] S.A. Idris, Adsorption, kinetic and thermodynamic studies for manganese extraction from aqueous medium using mesoporous silica, J. Colloid Interface Sci., 440 (2015) 84–90.
[41] S.K. Bajpai, N. Chand, M. Mahendra, The adsorptive removal of a cationic drug from aqueous solution using poly (methacrylic acid) hydrogels, Water SA, 40 (2014) 49–56.
[42] R. Abu-Zurayk, R. Al Bakin, I. Hamadeh, A. Al-Dujaili, Adsorption of Pb(II), Cr(III) and Cr(VI) from aqueous solution by surfactant-modified diatomaceous earth: equilibrium, kinetic and thermodynamic modeling studies, Int. J. Miner. Process., 140 (2015) 79–87.
[43] T. Bohli, A. Ouederni, N. Fiol, I. Villaescusa, Single and binary adsorption of some heavy metal ions from aqueous solutions by activated carbon derived from olive stones, Desal. Wat. Treat., 53 (2015) 1082–1088.
[44] M. Kobya, E. Demirbas, E. Senturk, M. Ince, Adsorption of heavy metal ions from aqueous solutions by activated carbon prepared from apricot stone, Bioresour. Technol., 96 (2005) 1518–1521.